AFRL-RX-WP-TP-2008-4326

PLASTICITY OF MICROMETER-SCALE SINGLE-CRYSTALS IN COMPRESSION: A CRITICAL REVIEW (PREPRINT)

Michael D. Uchic, Paul A. Shade, and Dennis M. Dimiduk

Metals Branch
Metals, Ceramics, and NDE Division

OCTOBER 2008

STINFO COPY

AIR FORCE RESEARCH LABORATORY
MATERIALS AND MANUFACTURING DIRECTORATE
WRIGHT-PATTERSON AIR FORCE BASE, OH 45433-7750
AIR FORCE MATERIEL COMMAND
UNITED STATES AIR FORCE

REPORT DOCUMENTATION PAGE

1. REPORT DATE *(DD-MM-YY)*	2. REPORT TYPE	3. DATES COVERED *(From - To)*
October 2008	Journal Article Preprint	

4. TITLE AND SUBTITLE	5a. CONTRACT NUMBER
PLASTICITY OF MICROMETER-SCALE SINGLE-CRYSTALS IN COMPRESSION: A CRITICAL REVIEW (PREPRINT)	In-house
	5b. GRANT NUMBER
	5c. PROGRAM ELEMENT NUMBER 62102F

6. AUTHOR(S)	5d. PROJECT NUMBER
Michael D. Uchic and Dennis M. Dimiduk (AFRL/RXLMD) Paul A. Shade (The Ohio State University)	4347
	5e. TASK NUMBER RG
	5f. WORK UNIT NUMBER M02R1000

7. PERFORMING ORGANIZATION NAME(S) AND ADDRESS(ES)		8. PERFORMING ORGANIZATION REPORT NUMBER
Metals Branch (AFRL/RXLMD) Metals, Ceramics, and NDE Division Materials and Manufacturing Directorate Wright-Patterson Air Force Base, OH 45433-7750 Air Force Materiel Command, United States Air Force	The Ohio State University	AFRL-RX-WP-TP-2008-4326

9. SPONSORING/MONITORING AGENCY NAME(S) AND ADDRESS(ES)	10. SPONSORING/MONITORING AGENCY ACRONYM(S)
Air Force Research Laboratory Materials and Manufacturing Directorate Wright-Patterson Air Force Base, OH 45433-7750 Air Force Materiel Command United States Air Force	AFRL/RXLMD
	11. SPONSORING/MONITORING AGENCY REPORT NUMBER(S) AFRL-RX-WP-TP-2008-4326

12. DISTRIBUTION/AVAILABILITY STATEMENT
Approved for public release; distribution unlimited.

13. SUPPLEMENTARY NOTES
Journal article submitted to *Annual Review of Materials Research*. PAO Case Number: 88ABW 2008-0623; Clearance Date: 20 Oct 2008. The U.S. Government is joint author of this work and has the right to use, modify, reproduce, release, perform, display, or disclose the work. Paper contains color.

14. ABSTRACT
This review examines the recent literature that has focused on uniaxial compression experiments of single crystals at the micrometer-scale. Collectively, the studies discovered new regimes of plastic flow that are size-scale dependent and that occur in the absence of strong strain gradients. However, the quantitative comparison of the flow curves between independent studies is hampered by differences in the particular implementations of the testing methodology. Two schools of thought have emerged regarding the observed size-scale effects; one attributes the effects to lack of dislocations in small samples, while the other attributes them to dislocation behavior in truncated volumes. The former, but its nature, lacks quantitative models. The latter has relied on modeling of the microcompression experiment using 3D discrete dislocation simulations, which has provided leading insight into the mechanisms that may control plastic flow in FCC metals. These efforts identified the importance of the initial dislocation density and distribution of mobile segments, as well as altered multiplication and hardening responses due to finite source statistics.

15. SUBJECT TERMS
size effects, microcompression testing, strength, strain-hardening, experimental techniques, discrete dislocation simulations, flow intermittency

16. SECURITY CLASSIFICATION OF:			17. LIMITATION OF ABSTRACT:	18. NUMBER OF PAGES	19a. NAME OF RESPONSIBLE PERSON (Monitor)
a. REPORT Unclassified	**b. ABSTRACT** Unclassified	**c. THIS PAGE** Unclassified	SAR	42	Christopher F. Woodward **19b. TELEPHONE NUMBER** *(Include Area Code)* N/A

i

Plasticity of micrometer-scale single-crystals in compression: a critical review

Michael D. Uchic[1], Paul A. Shade[2], and Dennis M. Dimiduk[1]

[1] Air Force Research Laboratory, Materials & Manufacturing Directorate, Wright-Patterson AFB, Ohio, 45433
[2] Department of Materials Science and Engineering , The Ohio State University, Columbus, Ohio 43210

Abstract

        This review examines the recent literature that has focused on uniaxial compression experiments of single crystals at the micrometer-scale. Collectively, the studies discovered new regimes of plastic flow that are size-scale dependent and that occur in the absence of strong strain gradients. However, the quantitative comparison of the flow curves between independent studies is hampered by differences in the particular implementations of the testing methodology. Two schools of thought have emerged regarding the observed size-scale effects; one attributes the effects to lack of dislocations in small samples, while the other attributes them to dislocation behavior in truncated volumes. The former, by its nature, lacks quantitative models. The latter has relied on modeling of the microcompression experiment using 3D discrete dislocation simulations, which has provided leading insight into the mechanisms that may control plastic flow in FCC metals. These efforts identified the importance of the initial dislocation density and distribution of mobile segments, as well as altered multiplication and hardening responses due to finite source statistics. Microcrystal experiments have also provided a new pathway to characterize the global system dynamics of dislocation ensembles. Topics that should receive further study include extending experimental methods to include other testing configurations and elevated temperature testing, the continued investigation of the correlation limits for mechanical properties, the statistical characterization of flow intermittency for a broad range of materials systems and testing conditions, and the further maturation of 3D simulation methods that examine aggregate dislocation behavior in small volumes.

Introduction

        Structures large and small are frequently designed to loads that exceed the elastic limit and thus require a reliable understanding of their time-dependent response to plastic processes. Today this is achieved by empirical testing of extracted samples at the macro-scale, or testing of full-scale devices at the sub-millimeter scale. For the

future, engineering design is beginning to demand structure-dependent models to enable quicker transition of novel advanced materials. However, the basis for mechanical analysis that spans different length scales remains heuristic since the influences of microstructure at the dislocation scales and larger are not yet well represented within plasticity or deformation theories or simulations. That is, neither the kinetics of dislocation structure evolution within material grains, nor the evolution of the plastic behavior of an aggregate of grains is understood at small length scales. Thus, one must measure, understand and model the responses to variations in microstructural features or the geometric scales of devices and create phenomenological representations of their effects for engineering design.

To better understand and advance the models of plasticity so that they may include the fundamental materials science of deformation at small scales, new experimental methods are needed that permit better coupling to all aspects of theory and simulation. Accordingly, about five years ago, some of the present authors introduced a new specimen preparation and compression testing technique for evaluating the flow properties of materials via specimens that range from sub-micrometer to several tens of micrometers in size. Even from the first experiments on micrometer-scale nickel single crystals it was clear that new intrinsic mechanisms operate when the physical dimensions of a sample approach those of the dislocation processes. Since those initial experiments, more than seventy papers have appeared in various journals that describe direct or derivative applications of the technique, extensions of materials science concepts that explain the observed phenomena and, simulation studies that mimic aspects of the results within bounded micromechanisms. This review critically examines a selected suite of these publications to assess growth in our understanding of plasticity in small volumes and to provide a succinct summarizing perspective on this rapidly expanding field.

The review is built within four parts. The first examines the test methodology and highlights potential issues that affect the experimental measurements. The second section reviews what has been done experimentally and focuses on key findings and limitations of the experimental studies. The third part treats the related theory, modeling and simulation studies that have built upon the experimental findings. The final part of the review offers some perspective on what has been learned, what it may mean for the science of crystal deformation, and what studies, in the view of the present authors, should be attempted in the near term so as to clarify selected uncertainties within the work to date.

Microcompression Methodology

We begin by briefly describing the microcompression testing methodology, which is shown schematically in Figure 1. This test mimics the compression experiment commonly performed on macroscopic samples, with some modifications to facilitate both the fabrication of the diminutive samples and their subsequent manipulation into the testing system (1-3). The most significant difference is that the micro-compression samples are not freestanding; rather, they remain integrally-attached to the bulk

substrate in order to eliminate the need for micromanipulation. As a result, the substrate acts as the lower compression platen during the test. Commercial nanoindentation systems are commonly used as the mechanical test frame, where the sharp indentation tip is replaced with a flat-punch tip. The load and displacement resolutions of most nanoindentation systems are well-suited for micro-compression testing, as they typically produce stress-strain curves with micro-strain and sub-MPa resolution for micrometer-scale samples (1). The specific performance parameters for each testing system naturally bound the range of sample sizes that can be interrogated.

Sample fabrication and associated concerns

The vast majority of microcompression samples have been fabricated via Focused Ion Beam (FIB) micromilling, which allows one to serially manufacture micro-compression samples into the surface of a bulk crystal with extreme control over both the location and size of the sample (1-3). Typical sample sizes range from a couple hundred nanometers to twenty micrometers in diameter, with sample fabrication times ranging from a couple of hours to multiple days. Note that other methods for sample fabrication include microelectronics-based processes that create arrays of metal (4) or semiconductor (5) pillars, and selective etching of directionally-solidified alloys (6).

The sample geometry produced by FIB milling can be separated into two classes. The first are samples that have been milled where the ion beam orientation is perpendicular to the bulk sample surface (7-12). These samples are easily produced by the FIB microscope with stock milling patterns, and therefore are more commonly used. However, the sample geometry produced by this method complicates the interpretation of the micro-compression experiments. The samples always have some degree of taper such that the diameter at the top is smaller than that at the base, and unless great care is taken, the gage length is not uniform and potentially can be much larger than the generally-preferred aspect ratio for single-crystal compression samples (length-to-diameter ratio between 2:1 and 3:1). The taper angle will vary with milling conditions, but is generally within 2 to 5 degrees.

The primary problem with tapered samples is that this geometry leads to a non-uniform applied stress field within the sample (in addition to other variations in the local stress field due to the test boundary conditions). The effect of taper has been studied analytically (11) and numerically by finite element modeling (FEM) (13). These studies showed that the tapered sample geometry results in inhomogeneous deformation, which can lead to inaccuracies in determining the flow stress and also produces an artificial increase in the strain-hardening rate. For example, a sample having a 4.5° taper and a 3:1 aspect ratio will have an applied stress in the middle of the sample that is 35% less than that at the top of the sample, and similarly the stress at the base is 55% less than at the top. Thus, the quantitative measurement of the flow stress and strain hardening behavior from experiments that utilize this geometry should be assessed critically with regards to these sources of error.

The second type of samples are prepared using a procedure called 'lathe milling,' where the ion beam is at an oblique angle to the bulk sample surface (1,3). While these

samples take more time and effort to produce, they have both a uniform cross-section and a controlled aspect ratio. In addition, lathe milling can be used to prepare samples that are either polycrystalline or polyphase, while the simpler milling methods may encounter problems with differential milling rates (14).

One concern associated with any FIB-prepared sample is the irradiation-damage layer that is created by the impact of highly-accelerated Ga^+ ions. The extent and thickness of this damage layer is dependent on a number of parameters, including the atomic weight and bonding characteristics of the target material, angle of the incident beam, ion energy, and the total dose to name a few (15-17). For some materials, there may be other considerations such as the precipitation of Ga-containing phases (18-19), and still other materials are prone to Ga-embrittlement.

Two independent studies by Motz et al. (20) and Bei et al. (21) examined the local surface strengthening effect of 30 kV Ga^+ implantation using nanoindentation hardness measurements. Both studies showed that the hardness of irradiated surfaces is higher than those that have not been irradiated for indent depths less than 300 nanometers, with the increase in hardness approximately a factor of 2 at depths less than 100 nanometers. However, those studies did not examine whether the strengthening due to surface irradiation damage, as measured via nanoindentation hardness measurements, translates into strengthening of microcompression test specimens.

The work of Greer and Nix endeavored to directly assess the effect of FIB-irradiation damage by examining Au microcrystals prepared by four different means: FIB milling, FIB milling followed by annealing, FIB milling followed by low-energy Ar^+ milling, and samples that were grown via electrodeposition followed by annealing (which produced microsamples that were typically composed of a few grains) (4,7). Thus, the degree of implantation damage was presumably different for the four processing routes, with the as-FIB prepared surface having the most damage. Their experiments showed that the micro-compression flow-stress values for the three different FIB-based processing routes had similar values, while the electrodeposited microsamples were stronger on average but showed similar size-dependent strengthening trends. Unfortunately, this study did not provide evidence of changes to the outer surface of the microcrystals for the various processing routes, save for determining that the low-energy Ar^+ mill decreased Ga concentration at the surface. Nonetheless, based on these results Greer and Nix concluded that the strengthening effect due to FIB-irradiation damage was negligible.

Another study that examined irradiation-damage defects was the work of Shan and co-workers using in-situ TEM mechanical tests (11). This study showed that most, if not all, of the dislocation substructure—including the irradiation-defects—disappeared from sub-micrometer diameter micro-crystals upon loading, a process they termed 'mechanical annealing.' The authors found that the reduction in total dislocation density was related to the sample diameter. Smaller samples (< 200 nanometers in diameter) became dislocation-free upon straining, while larger samples (up to 400 nm in diameter) qualitatively retained some dislocation density. However, the authors did not

4

provide any quantitative information as to the stresses at which significant reductions in the small-loop dislocation density occurred.

In summary, there is a well-documented and straightforward approach for preparing micro-compression samples via FIB microfabrication. Mechanical test data produced using tapered samples should be viewed critically with regards to potential artifacts in the stress-strain curves. At this time, the thin irradiation damage layer produced by FIB milling does not appear to strongly influence mechanical properties and, over selected size regimes, has been shown to disappear upon loading, although more definitive studies in this area are needed.

Mechanical testing and associated concerns

There are additional considerations for performing accurate micro-compression experiments. For example, the elastic deflection of the integral substrate must be accounted for if one is interested in obtaining accurate modulus values. Methods to correct for substrate deflection have been developed both analytically and numerically (7,13,22). A primary practical concern is to ensure that there is minimal misalignment between the flat-punch tip (platen) and the top surface of the sample. Misalignments, especially those that are greater than 1°, lead to a number of test artifacts: underestimation of the yield point and elastic modulus, changes to the strain-hardening response, and buckling (13,22). A method for minimizing misalignment has been introduced by some of the present authors (3) that is qualitative in nature, and further improvements in this area are needed. As with tapered microcompression samples, experiments that do not attempt to correct for misalignment may have artifacts present in the data.

Another influence of the test apparatus is more subtle, which is related to the integral connection of the microcompression sample to the substrate. In the traditional compression experiment, ensuring adequate lubrication between both platens and the sample is good experimental practice. However, for the microcompression experiment, the bottom end of the sample is rigidly constrained, thus the test boundary conditions can be different than a well-lubricated bulk experiment. Indeed it is the triaxial base constraint that enables integral specimen compression testing without significant plasticity within the bulk substrate. Importantly, it is the ability of either the top of the specimen to slip against the indentation platen or for the platen to laterally translate during an experiment that can greatly affect the stress-state within the sample. The experience of the present authors, using in-situ scanning-electron microscope deformation experiments (where lubricants are not used), suggests that the sample does not slide along the platen surface during deformation; rather, the platen-and-sample move laterally as a conjoined unit (23).

One issue related to the lateral movement of the top sample surface during a microcompression experiment is plastic instability (buckling). Zhang (13) and Raabe (24) studied this aspect of testing using isotropic continuum FEM and anisotropic crystal-plasticity FEM, respectively. Both studies show that plastic instabilities occur at lower strain values for samples having either larger length-to-diameter ratios or lower platen-

to-sample frictional coefficients. Raabe also selectively studied the effect of crystal orientation and showed that crystals near but not exactly parallel to the symmetric [001] orientation, display plastic instabilities at smaller strain values compared to more stable multi-slip orientations (24). Nevertheless, these studies show that even for the most extreme circumstances (single-slip orientation and zero friction), the flow curves for samples having a 2:1 to 3:1 aspect ratio are not strongly affected by plastic buckling until the engineering strain exceeds a value of 5%.

Conversely, while friction or lateral-constraint is beneficial to prevent plastic instabilities, the uniformity of the internal stress field can be strongly affected by this constraint. Recently, the present authors and co-workers demonstrated using both experiments and crystal-plasticity FEM analysis that varying the lateral constraint of the test system affected the following phenomena: the uniformity of the internal stress field, the measured flow stress, the observation of 'large' strain bursts, the development of local internal gradients and, the strain-hardening behavior (23). Some of these effects are highlighted in Figure 2. Thus, knowledge of the lateral resistance of the micro-compression test system is beneficial, in the sense that the observation or absence of particular physical attribute(s) may be directly influenced by this constraint.

Another comment regarding mechanical tests is that in surveying the literature there are some differences in the testing modes that are performed, which in some cases can be traced to the type of test system that is employed and whether it is inherently a stroke- or load-controlled device.   Examples can be found of either constant displacement-rate testing (4,11), constant loading-rate testing (9), or a hybrid method that contains periods of both constant displacement rate and creep holds (3). Note that the choice of testing method for microcrystals may have more of an effect on the stress-strain behavior as compared to bulk-crystal testing because microcrystals often display strain instabilities, i.e., strain avalanches. A true constant displacement-rate test will damp out strain bursts and produce a serrated stress-strain curve, whereas a constant loading-rate method may accentuate the magnitude of strain bursts. Systematic suppression or enhancement of these events should lead to measurable differences in the strain-hardening response and, may also bias the statistical attributes of strain bursts.

To date, typical microcompression experiments span quasi-static strain rates ranging from 10^{-3} to 10^{-6} s^{-1}. All reported tests have been performed at room temperature. The effect of thermal activation on small-scale deformation remains an open question, although commercial nanoindentation devices have been demonstrated to operate at elevated temperatures (26).

Observation of physical phenomena

FCC metals

Many of the initial applications of the micro-compression methodology focused on studies of simple metals; in particular, elements that possess the Face Center Cubic (FCC) crystal structure. The reasoning for this is two-fold: the single-crystal flow

behavior of these metals has been studied in great detail by testing of both bulk samples and vapor-grown whiskers and, similarly, there is extensive knowledge regarding the active dislocation processes and structures that result from plastic deformation. In addition, the use of Au crystals enables the study of small-scale deformation in a material that does not form a native oxide layer.

The phenomenon that has garnered the most attention for experiments on FCC microcrystals (micrometer-scale single crystals) of pure Ni (2,11,25,27), Au (4,7-9), Al (12,28), and Cu (28-30) is the strong dependence of the flow stress on sample size when the sample diameter is of the order of tens-of-micrometers or smaller. This increased flow stress results from both increases of the proportional limit and, tremendous strain hardening at micro to moderate strains, at rates that are often greater than Stage II hardening (25,34). In fact, for some experiments the overall strain-hardening rate over this regime is a large fraction of the elastic modulus (25). Following this micro-plastic regime, the strain-hardening rate decreases rapidly and the flow stress typically remains constant or increases much less rapidly for the remainder of the test.

This enhanced strain hardening at small strains is size-scale dependent, with smaller samples exhibiting higher strain-hardening rates (9,25,27). As a result, pure-metal crystals that have sub-micrometer diameters can achieve incredibly high flow stresses. For example, reports show that approximately 200 nanometer diameter <111> oriented Ni microcrystals strain harden and ultimately sustain stresses of 2 GPa and higher (11,27). Conversely, 20 micrometer and larger <269> microcrystals display strain-hardening rates that are equivalent to Stage I flow in bulk crystals (25). Unfortunately, the use of tapered specimens in many of these studies precludes the quantitative comparison of the strain-hardening rates, due to the spurious strain hardening associated with this sample geometry (13).

The size-affected yield and strain-hardening response is also stochastic. Close inspection of the flow curves in this region reveals a binary mechanical response, composed of either periods of elastic or nearly-elastic loading separated by strain bursts where no strain hardening takes place. The strain bursts occur at random intervals at stresses above some critical value, and the magnitude of these events is also random, although these statistics are governed by global system dynamics as discussed later on.

In the regime where size-dependent strengthening is observed, the relationship between flow stress (σ) and sample diameter (d) can be empirically described by a power law:

$$\sigma = A d^{-n} \qquad \qquad 1.$$

where A is a constant, and n is the power-law exponent. Generally this relationship holds for sample diameters that range from a couple hundred nanometers to tens-of-micrometers in diameter. The power law exponent for FCC metals varies from study to study, ranging from 0.61 (9) to 0.97 (31also Ng & Ngan). These values are different than those typically associated with grain-size strengthening (n = 0.5) or surface-controlled nucleation (n = 1), for example. Note that the value of n in Eq. 1 is dependent on the absolute magnitude of the stress at a given sample diameter, e.g., for a fixed change in stress over a given size range, the value of n will decrease as the absolute values of stress are increased. The strain value at which the flow stress is determined varies from

study-to-study as well, ranging from the proportional limit (12) to 10% strain (7,8). This variability may be attributed to an attempt to find a saturation stress on some portion of the stress-strain curve, where the scale-affected strain-hardening behavior may be artificially extended due to the use of a tapered sample geometry or sample misalignment.

All of the pure-metal FCC size-dependent strengthening data can be collapsed onto a single band by plotting a normalized resolved shear stress versus sample diameter, where the flow stress is normalized by the shear modulus and relative ratio of the Burgers vector of each metal as shown in Figure 3. This figure shows that a scaling exponent of 0.6 is a reasonable match to much of the data. However, this agreement is perhaps fortuitous. As will be discussed later, recent experiments on pre-strained Mo microcrystals by Bei et al. (32) and 3D discrete dislocation simulations (DDS) by Rao et al. of FCC microcrystals (33) show that the degree of size-dependent strengthening is dependent on the initial dislocation density. One possibility is that the elemental materials examined by five different independent studies contain similar starting densities. In three of the studies, this condition is met, as the initial starting densities are reported to be of the order of 10^{12} m^{-2} for two of the studies (12,27) and moderately higher in a third (25,34). Another explanation is that a double logarithm plot is not ideal for discerning subtle differences among data.

Size-dependent strengthening is observed in both single-slip (2,9,12,25) and multiple-slip orientations (7,8,27,30). Note that there has been no experimental microcompression study of the same bulk crystal tested under both symmetric and single-slip orientations, thus the quantitative effect of crystal orientation on the size-dependent flow response is unknown. That being said, the relative importance of crystal orientation lessens as the sample diameter shrinks to the micrometer scale, as the stress-strain curves for both single-slip and multiple-slip orientations become qualitatively similar when size-affected strain hardening dominates plastic flow.

BCC metals

Measurements of Body Center Cubic (BCC) metal plasticity using microcompression testing is limited to pure Mo and Mo solid-solution single crystals. In general, the behavior of FIB-prepared BCC microcrystals is similar to FCC microcrystals with regards to the size-dependent strengthening response. As the sample size is diminished, the strain-hardening behavior at small strains displays a size-affected response, as demonstrated in Figure 4. As a result, the flow stress measured at finite-strain values also increases with decreasing sample size. This has been determined for both symmetric (6,31,32,35) and single-slip orientations (35,36). Unlike FCC microcrystals, the slip traces observed on Mo microcrystals appear to be much more finely distributed along the gage length (36).

The recently-published study of Bei and colleagues on Mo alloy microcrystals is noteworthy (6,32). These microcrystals were produced from selective etching of a two-phase aligned eutectic microstructure wherein the phase-of-interest, a Mo(Ni,Al) solid solution, solidified as directionally-aligned whiskers within a NiAl(Mo) matrix.

Advantages of this fabrication method include the following: FIB-based processes are not needed to create the microcrystals and therefore the outer surfaces are not irradiation-damaged; microcrystals are created in parallel, thereby allowing for sufficient measurement statistics; the bulk composite crystals can be deformed to various amounts prior to etching, which allows for the systematic study of the effect of the initial dislocation density on microcrystal deformation.

A summary of the results from this study is shown in Figure 5 (32), which highlights two important findings. First, this study rather conclusively shows that an increase in initial starting dislocation density actually *softens* microcrystals, which is contrary to bulk-crystal behavior. Microcrystals that are presumed to be defect-free display an incredibly high yield stress (9.3 GPa), which decreases dramatically when an initial dislocation substructure is present in the microcrystals. Similarly, microcrystals that are prepared from a bulk-crystal deformed to 4% strain are on-average stronger than those prepared from an 11% strained bulk crystal. Second, the observation of size-affected behavior is directly dependent upon the starting dislocation density. At the extremes—either dislocation-free or for sufficiently high starting densities—the microcrystal deformation behavior is independent of the size of the sample volume. Also, at either extreme condition the scatter in the flow stress is relatively small, and for the high-density crystals the flow curves are smoothly varying and strain bursts are generally absent. Only at intermediate dislocation densities are a size-dependent strengthening and stochastic flow response observed.

Other materials

A recent study by Nadgorny and some of the present authors examined the behavior of LiF crystals that differ from the FCC and BCC microcrystal studies beyond the obvious differences in active glide systems (37,38). First, the bulk crystals are highly pure and almost defect-free, having a starting dislocation density less than 10^9 m^{-2}, which is much less than the densities reported for FCC microcrystal tests. Second, some of the crystals were irradiated by γ-rays that produce a well-known and dense array of pinning points throughout the crystal volume. Third, the behavior of dislocations in alkali halide crystals has been thoroughly investigated. As a result, these materials potentially offer a more-controlled approach to examining size-scale effects. Subsequent testing of both crystal types showed that the microcrystal deformation response is strongly size-affected. The power law scaling exponent is higher than that found for the majority of FCC microcrystal studies, which likely is attributed to the low starting dislocation density. A somewhat surprising result was this enhanced small-strain-hardening behavior overwhelms any differences in internal structure.

Due to space restrictions this review cannot fully comment on the entirety of microcrystal or microcompression testing work that has spanned a wide range of materials systems and advancement in test methodologies. A list of these activities include microcompression testing of shape memory alloys (39,40), nickel superalloys (3), titanium alloys (40,41), Ni$_3$Al intermetallics (2,41,42), Cu/Nb nanolaminates (43), nanocrystalline Ni (42,44,45), metallic glasses (46-48), stainless steel (49), nanoporous

Au foams (50), in-situ testing of silicon (5) and gallium arsenide (51), creep testing of Al microcrystals (52), bend testing of Cu microcrystals (53), and tension testing of Cu microcrystals (29,54).

Intermittency

In addition to size-scale strengthening effects, another almost-universally observed phenomenon in microcrystals is an intermittency associated with plastic deformation. Unlike bulk-crystal deformation, which is usually associated with smoothly-varying flow curves, discrete bursts of strain activity are regularly observed in microcrystal flow curves, as shown in Figure 6. The stress-strain curve of a 20 micrometer diameter Ni microcrystal deformed to 20% strain is usually comprised of many hundreds or even thousands of discrete events (55).

Intermittency of plastic flow for large samples has been previously characterized through other means (image-based analysis of slip trace evolution (56) and acoustic emission experiments (57), for example). The observation of strain bursts in microcrystal experiments provides a means for direct quantitative measurements of the statistical attributes of such events. The strain bursts have typical magnitudes that are of the order of Angstroms to micrometers (12,31,55). The limited sample volume associated with the microcompression experiment—in conjunction with nanometer-per-second displacement rates and sensors that provide sub-nanometer displacement resolution—facilitate the measurement of dislocation bursts by minimizing the probability that multiple events will take place at the same time. As a consequence, this methodology provides a unique means to directly measure the total displacement associated with each event, the time duration for each event, and the time between events.

The quantitative study of the size of slip events using the microcompression test was first performed by some of the present authors and colleagues (42,55), and also later by Csikor (58), Brinckmann (31), Ng and Ngan (12), and Zaiser (35). These studies all agree that the number and magnitude of slip events display a power-law scaling (with a cut off), in some cases spanning event sizes that range over three-orders of magnitude. This power-law scaling is described by the following equation (58):

$$n(x) = C\,x^{-\alpha}\,\exp[-(x/x_0)^2] \qquad\qquad 2.$$

where $n(x)$ is the probability of an event of magnitude x, C is a constant, α is the power law scaling exponent and, x_0 is the characteristic magnitude of the largest avalanche. The value of α is reported to be approximately 1.6 for much of the experimental data published to date (12,31,35,55,58), but one study showed that this value is dependent upon the applied strain rate (42). The procedure for cataloguing the number of events and their magnitudes is beyond the scope of this review, but note that these methods require improvement for quantitative analysis and should be approached cautiously. For selected studies, changes in the parameters used in the analysis lead to differences in the event distributions and measured scaling exponents (61) or, were found relatively insensitive to these changes (35).

There are other attributes in addition to so-called scale-free flow associated with dislocation bursts: the events transpire at rates much faster than the applied driving force; large events often occur after only a small change in the applied stress, i.e., the dislocation ensemble is at a near-critical state; large events are often followed by smaller events during periods of constant driving force, analogous to the shock-aftershock behavior observed in earthquakes; large multitudes of dislocations are able to participate in deformation (55). Collectively, these characteristics place dislocation-mediated flow as having the same global system dynamics as plate tectonics, sand pile avalanches, and other dynamical systems that are described by the term "self-organized criticality." Although these types of experimental studies are only in their infancy, the discovery of this behavior has current practical implications on plastic forming at the micro-scale (58), and long-term implications on the development of new meso-scale deformation theories that accurately predict the group dynamics of dislocation ensembles (55).

Characterization of the internal structure in microcrystals

The following section discusses experimental studies that characterized the change in internal structure during microcrystal experiments. To date, two different methods have been used to gather information and help shed light on the mechanisms responsible for size-scale strengthening effects: transmission electron microscopy (TEM) and micro-focus x-ray diffraction.

The majority of studies that used TEM focused on preparing site-specific foils from deformed FCC microcrystals, in order to observe any internal changes that occurred after testing. The works of Greer and Nix (4), Frick and colleagues (27), and Ng and Ngan (12) used TEM foils for which the foil plane is a vertical cross-section of the microcompression specimen that contains the centerline axis of the microcrystal. By comparison, the study by Norfleet and co-workers (34,40,41) primarily examined foils that enveloped primary slip traces. Note that the mottled contrast (as a result of irradiation damage) and foil bending that is often observed in FIB-prepared TEM foils can make the resultant images more difficult to interpret.

On the surface, the findings of these TEM studies are somewhat contradictory. Some of these differences may be attributed to the foil plane, and also to the size and orientation of the deformed microcrystal that was investigated. Both the studies by Greer and Nix and Ng and Ngan conclude that the only residual dislocations observed in sub-micrometer <001> Au and <315> Al crystals, respectively, after deformation are those that belong to unfavorably-oriented slip systems (4,12). The Ng and Ngan study also examined 6 micrometer diameter single-slip oriented Al crystals and determined that the dislocation density increased only a slight amount after moderate straining, and no evidence was observed of dislocation patterning (12).

These observations are consistent with the novel in-situ TEM study by Shan and co-workers, that shed some additional light on deformation processes in sub-micrometer <111>-oriented Ni crystals (11). As mentioned previously, the phenomena of 'mechanical annealing' was discovered in these experiments, where the initial

11

dislocation density decreased significantly upon loading and, at the limit of extremely small sizes (sub-200 nanometer diameter), the microcrystal becomes completely defect-free. However, slightly larger-sized crystals still maintained some stored density, even at stresses as high as 2.6 GPa. Also, after the period of mechanical annealing, further plastic flow was reported to be accommodated through dislocation nucleation.

By comparison, Frick and colleagues observed an increase in dislocation density for deformed sub-micrometer <111> Ni crystals, but they did not quantify the change in the stored density (27). This study also found small changes in the lattice orientation of the deformed microcrystals relative to the substrate, which were less than 3°. The work of Norfleet and colleagues examined slip traces and bands in <269> Ni microcrystals that ranged in size from 1 to 20 micrometers in diameter (34). Their study reported the following findings: dislocation structures in slip bands were qualitatively similar to those found in bulk crystals during Stage I flow; on average, the stored density in slipped regions was higher than the initial density, especially for samples that exhibited strong size-affected strain hardening; the increase in density occurred at early stages of plastic flow, remaining nominally constant thereafter; significant dislocation-activity occurred on non-primary slip systems, even though the microcrystals were oriented for single-slip; Also, both the rise in density and bulk-like slip patterning were not observed when these same experiments were performed on vertical cross-section foils, suggesting that dislocation activity and organization is highly-localized (62).

The micro x-ray diffraction (XRD) studies offer a complementary and non-destructive means to assess local changes in internal structure, especially allowing one to examine for changes to the excess dislocation density, or local lattice distortions, without altering the microsample geometry; however, only a few studies exist. Budiman and co-workers performed micro-XRD measurements before and after a microcompression experiment and their lattice curvature measurements determined that there were no more than 3-4 excess dislocations existing within a 580 nanometer diameter Au crystal deformed to 35% strain (63). Again, the technique is insensitive to redundant or multipolar stored dislocations. These results are consistent with the TEM studies of Greer and Nix, Ng and Ngan, and Shan and colleagues (4,11,12).

The group of van Swygenhoven has also examined microcrystal deformation using micro-XRD measurements (64-68). They employed a custom in-situ testing system that enables the collection of local diffraction pattern changes throughout the mechanical test. Studies have been performed on Au, Cu, and Ni microcrystals prepared by a number of independent research groups, and the collective findings from these efforts include the following: FIB-prepared microcrystals can contain pre-existing defects that result in internal lattice distortions (strain gradients) (64,65) or low-angle boundaries (65,66); deformation can occur on non-favorably oriented slip systems for smaller microcrystals, where selected slip activity may be correlated with the presence of local gradients (67); if initially present, local rotations and gradients evolve during deformation (68); some local gradients appear to intensify prior to a strain burst, and then diminish after the event (67). Still, the connection between these observations of dislocation-ensemble activity and the phenomena of size-affected strengthening is not well-established.

Taken as a whole, the TEM and micro-diffraction studies infer a picture of dislocation mediated flow where—especially for sub-micrometer crystals—the storage and patterning of dislocations can be strongly affected. However, at larger scales, the evidence suggests that more bulk-like dislocation substructures evolve on active slip planes, but other aspects of patterning might be altered by the limited sample volume. Still, further study in this area is much needed, especially across the wide diversity of materials that exhibit size-affected flow.

Bulk Properties

One aspect of size-affected flow that has received less-attention is the dimension at which one transitions from 'size-affected' to 'bulk' properties. All studies, except those by the present authors, fabricated samples where the diameter is 10 micrometers or smaller. This is principally because the FIB milling times for samples increase dramatically for samples larger than this size. The studies of Ni, Mo, and Ni-base superalloy microcrystals by the present authors show that the transition to bulk-like flow behavior—determined by direct comparison of microcrystal flow curves to macro-compression experiments of the same bulk crystals—occur at surprisingly large crystal sizes, i.e., diameters of 20 micrometers and larger (25,36,69). In addition, the flow stresses for all of the microcrystal experiments are almost always higher than their bulk counterparts, even for microcrystals as large as 80 micrometers in diameter (36,69). Given the relative lack of effort to date on this issue, characterizing the transition to bulk properties as a function of crystal type and internal dislocation substructure remains a worthy topic of study.

Theory or simulation of observed phenomena

This section examines theoretical and simulation efforts to understand the variety of phenomena observed in microcompression experiments, in particular the size-dependent flow stress, strain-hardening rate and flow intermittency.

Dislocation Starvation

One of the first explanations for the size-dependent strengthening of microcrystals was advanced by Greer and Nix, which is called the 'dislocation starvation' model (7,70,71). This model accounts for a change in plastic deformation behavior with sample volume by examining the relative rates of dislocation multiplication and dislocation escape. Essentially, this model states that behavior of small crystal volumes will be affected when mobile dislocations prematurely annihilate at the nearby free-surfaces rather than multiply via double cross-slip and similar processes. Thus, when the crystal dimensions (d) are some small multiple of the dislocation multiplication or breeding distance (δ), mobile dislocations leave before replicating and, this ultimately leads to a state of mobile-density starvation. Once the mobile density is extinguished, the stress needs to be raised significantly in order to nucleate dislocations either in the

bulk or at the surface. An analytical formulation for the starvation mechanism has been developed (70,71), but as-constructed the model only accounts for a single, finite-strain displacement event followed by elastic loading, and does not attempt to model the remainder of the size-affected flow curve. Nonetheless, the notion of 'starvation' dominated published findings in this field until the results from 3D discrete dislocation simulations (DDS) began to circulate and draw discussion.

2D Discrete Dislocation Simulations

The first simulation efforts to examine athermal microcrystal flow employed 2D discrete dislocation simulations. These simulations reduce the complexity of tracking dislocation motion by representing dislocations as infinite-line singularities that are intersected by a planar simulation cell oriented normal to them (72). One consequence of this simplified representation of intrinsically 3D dislocation mechanisms is that rules must be constructed to infer 3D phenomena such as source expansion, motion, annihilation, junction formation and their associated strengths, obstacle distributions, etc. into the 2D frame-of-reference. Obviously, the details regarding the formulation of these rules can have a strong effect on the outcome of the simulation, especially if salient deformation characteristics are not accurately represented or missing (for example, the distribution of source segments with sample size).

Deshpande and colleagues examined the uniaxial deformation of 2D simulation cells where only one slip system was operative, studying cases of both constrained and unconstrained flow (73-75). In these studies, the mean and variance of the dislocation source strengths, an obstacle spacing and obstacle strength were selected to be independent of the simulation cell size. For unconstrained simulations, these studies calculated a size-dependent response that consisted of an upper yield point followed by flow softening that intensified with increasing cell size. Notably, this behavior is not observed in experiments.

The size-dependency displayed in these 2D DDS can be attributed to dislocation pinning and, subsequent pile-ups were more likely to occur in larger cells, which resulted in stronger local fluctuations of the stress field that lowered the applied stress needed to sustain plastic flow. Accordingly, when dislocation pinning was not allowed to occur, the magnitude of the size-dependent softening response was lessened. Conversely, in the constrained simulations, almost no size-dependency was observed, as all cells regardless of size displayed flow softening behavior. In the constrained simulations, all cells were able to establish internal dislocation-density gradients in order to satisfy the boundary conditions, thus locally-augmenting the internal stress field and mobile segment population.

Benzerga and colleagues also used 2D DDS to investigate size-effects that arose from microcompression testing (76,77), where these models included different rules for the effects from junction formation and, source or obstacle creation. In contrast to the Deshpande et al., investigations, each dislocation source was randomly assigned a length, where the maximum possible length was dependent upon the cell size (76). These 2D DDS displayed a size-dependent increase in the proportional limit with

decreasing simulation cell size, which was attributed to the change in the source activation stress for the few largest sources in any given cell. That is, the simulated material strength was directly related to the weakest source. However, while most simulated stress-strain curves displayed little-to-no strain-hardening after initial yield, in smaller cells dislocation pinning and subsequent blocking of sources produced strain-hardening rates that approached the elastic limit. A related cumulative response of weakest-source activation followed by enhanced hardening behavior due to the paucity of available sources was also observed in selected 3D DDS simulations, which will be discussed later.

A second study (77) used a dislocation source distribution similar to the Deshpande studies described above. These simulations did not produce a size-dependent change of the initial flow stress, but rather exhibited Stage I-Stage II flow curves where the Stage II strain-hardening response was size-affected. Similar to the Deshpande study, the overall simulation-cell response is unlike most experimental data, especially with regards to the change in strain-hardening behavior at initial yield.

In summary, while 2D DDS studies demonstrated a size-effected flow stress or strain-hardening rate, they are so far unable to reproduce the relevant qualitative aspects of experimental microcrystal stress-strain curves. The work of Benzerga and Shaver (76) stands out as having identified size-affected proportional limit strengthening behavior that is in qualitative agreement with 3D DDS results and current understanding of most experiments. It is possible that the utility of 2D simulations at the microscale will be improved with constitutive laws that have been informed from theory or 3D DDS.

3D Discrete Dislocation Simulations (3D DDS)

There have been a number of efforts to study the FCC microcrystal deformation experiments using 3D DDS (33,58,78-83). The 3D DDS has some significant advantages over the aforementioned 2D DDS, such as the local interactions between dislocations can be naturally accounted for and, the motion of dislocations, especially those that interact with the free surfaces of the microcrystal, can be more accurately modeled.

However, at present even the 3D DDS fall short of quantitatively mimicking the microcrystal experiments. Like the 2D DDS, the applied strain rates are approximately 10^4 to 10^8 times faster than those for the experiments. While these high rates are used for computational viability, their influence on dislocation interactions and substructure evolution are unexplored. Perhaps most importantly, there are selected aspects of dislocation-mediated plasticity that are implemented in an ad-hoc manner. One particularly crucial factor pertains to the initial dislocation substructure, especially with regards to the number, size, and distribution of dislocation sources. Note that all of the simulations contain moderate (~10^{12} m^{-2}) to high (10^{14} m^{-2}) dislocation densities that are similar to those found in the microcrystal experiments. As highlighted by the following discussion and in spite of their shortcomings, the results from state-of-art 3D DDS made a profound impact on the present understanding of microcrystal deformation.

Nearly all of the 3D DDS studies instantiate the initial dislocation density as a set of Frank-Read sources (FRS) having rigidly-fixed ends. However, the strength and

distribution of the initial FRS vary significantly from study-to-study. For example, the FRS may have a single fixed length with little or no variance that in some cases is much smaller than the sample dimensions (78,80,82), or these can have a random distribution of lengths whose upper bound is determined by the sample dimensions (33,81). Similarly, the FRS can be distributed evenly among all possible slip systems (78,80,82), randomly-distributed (33), or placed only on one slip system (81). The recent study by Tang et al. differs in that the initial source distribution is not pre-defined; rather, it is established by loading the simulation cell with a fixed density of straight and jogged dislocation lines that reconfigure after relaxing the system at zero applied stress (83). Other differences between studies include the following: whether or not cross slip is allowed, whether or not the influence of the free surfaces and the test boundary conditions are included in the model, the magnitude of the applied strain rate, the loading mode, crystal orientation (multi- versus single-slip), sample aspect ratio, and sizes of the simulation volumes.

Nonetheless, there is general agreement among these independent studies regarding the observation of size-dependent strengthening dominated by 'weakest links', significant hardening at small strains and intermittent flow, in agreement with the experimental results. The scaling exponent for size-dependent strengthening was determined in selected studies and these values are also similar to those observed in experiments, as shown in Figure 7a.

While there is concurrence on the development of a size-dependent strengthening response, the rationalization of this effect differs between the various studies. Tang and colleagues initially attributed this strengthening to simply an increased probability of dislocation escape from the smaller crystals, thus requiring an increase in stress to maintain sufficient mobile dislocation density (78). Senger and colleagues (82) ascribe the size-dependent strengthening to the size distribution and available number of sources. In their simulations, they observed flow softening for "larger" cells (up to 2 micrometers) as a result of creation of new sources that are longer than the initial distribution from dislocation reactions. Again, flow softening has not been observed in experiments on FCC microcrystals to date. For smaller simulation cells, Senger et al. observed strengthening effects related to a finite FRS population, which will be discussed in more detail shortly.

By comparison, Rao and colleagues (33,79) attribute the size-dependent strengthening to two new size-dependent phenomena. The first is a refinement of the source strength distribution due to the proximity of free surfaces, a process termed 'source-truncation' hardening (79). The refinement occurs during the initial operation of a FRS, where the interaction of the source with the nearby free surfaces creates two single-arm sources, often having minimum arm-lengths that are smaller than the original FRS. Rao's simulations show that the repeated operation of these single-arm sources accounts for almost all of the plastic strain generated in the simulation cell, therefore the length of the largest single-arm source (or sources depending on the strain rate) sets the flow stress in these simulations (33). This same mechanism is also observed to operate in the studies by El-Awady et al. (81) and Tang et al. (83). Both

Rao's and El-Awady's simulations contain widely dispersed initial FRS lengths, in contrast to other studies.

The other new size-dependent mechanism identified by the three independent groups of Rao et al., Senger et al., and Tang el al. is related to the paucity of dislocation sources in microcrystals within an environment where 3D dislocation reactions can take place (33,82,83). Unlike bulk crystals where there are typically a boundless number of potentially mobile dislocation segments (ready multiplication), the finite number of available mobile segments in microcrystals results in an altered strain-hardening response when a source stops operating due to typical forest-hardening processes. That is, the stress required to activate the next-weakest source after an obstacle encounter, may be much larger than would be required in bulk crystals because there is insufficient multiplication of mobile segments at the lower stress. Those altered probabilities of occurrence for weak links in the dislocation microstructure can result in much more potent average strain-hardening rates, especially in the small-strain regime. Thus, the flow behavior in source-limited microcrystals proceeds via the sequential activation and obstruction of the weakest sources, and this process is termed 'exhaustion hardening' (25,33).

Rao's study clearly shows that the size-dependent scaling response is directly dependent on the initial FRS density, where a higher starting density results in a weaker scaling response and vice-versa, as shown in Figure 7b. At large simulation cell sizes, normal forest-hardening processes dominate and simulations having a higher initial FRS density display a larger flow stress. This trend is completely reversed at smaller sizes, as higher-density simulations exhibit a lower flow stress with considerably less scatter compared to low-density simulations. Thus, the size-scaling response levels out with an increase in density because larger crystals become stronger and smaller crystals become weaker. These findings correspond favorably with the experiments on pre-strained Mo microcrystals by Bei and colleagues (32).

The combination of source-truncation and exhaustion hardening also convincingly accounts for the stochastic flow commonly observed in small-cell simulations (33,58,79-83). For the same starting density, different instantiations of the FRS distribution result in changes to both the distribution of largest single-arm source lengths, as well as the probability that a dislocation reaction will block the operation of these largest sources. It naturally follows that the resultant flow curves will vary randomly with these local rearrangements. Also, at a fixed density the stochastic response becomes more pronounced as the microcrystal size decreases, as there are potentially fewer sources that can operate at nearly the same stress, thereby maximizing the influence of any individual source.

In summary, these 3D simulations all point to a change in material response from bulk crystals that are governed by the kinetics of forest-obstacle formation, to a source/multiplication limited regime when the sampled volume falls below the correlation length of the dislocation forest as it is classically described (84,85).

Weak-link statistics and the correlation length

As discussed above, self-consistency of results from the 3D DDS suggests a strong dependence of the small-strain plastic response on the statistics of dislocation sources: number density, distribution per slip system, and stress required to operate said sources. There has been recognition from a number of independent groups regarding these statistical processes.

The study of Parthasarathy et al. developed a statistical model for the flow strength of microcrystals, which was heavily influenced by observation of single-ended source operation in the 3D DDS (86). Their statistical model sought to calculate the increase and variation in critical resolved shear stress (CRSS) by determining the stress required to activate the weakest single-ended source in a microcrystal when only one slip system is active. Analytical expressions were developed to predict the mean and variance for the longest single-ended source in a microcrystal as a function of sample diameter and initial density. The resultant source operation stress was added to the Peierls stress and the stress expected from the grown-in dislocation forest in order to calculate the CRSS of Ni and Au microcrystals, as shown in Figure 8. On this figure one can see that at the micro-scale the source operation stress becomes a dominate factor in determining the CRSS. Also, the decrease in the number of single-ended sources with shrinking sample volume results in greater statistical scatter of the CRSS. The predicted values of CRSS also agree well with experimental data on Au and Ni microcrystals.

Ng and Ngan constructed a statistical model (87) that adds additional complexity to that of Parathasarthy et al. (86). This model examines the minimum stress required to activate a single-arm source on any of the possible FCC slip systems for a single-slip oriented sample, thus accounting for the possibility of that initial slip activity will occur on a non-favorably oriented slip system (87). Like the Parthasarathy et al. study, the operating or yield stress for a sample is simply the minimum stress to overcome the sum of the Peierls stress, the single-ended source operating stress, and a forest hardening stress, where the geometrical-orientation of the slip systems and possible differences in the forest hardening stress between slip systems are also included in the calculation. While this study also demonstrates a size-dependence of the yield stress, a more notable finding is that the simulations quantitatively agree with experimental observations of slip trace activity in lightly-deformed Al microcrystals (87), as shown in Figure 9. Here, the observation of initial slip activity on a non-favorably oriented slip plane increases with decreasing microcrystal size. Therefore, the authors of this study conclude that Schmid's law, which states that plastic flow will occur on the slip system with the largest Schmid factor, no longer holds for microcrystal deformation.

Ng and Ngan also developed a phenomenological Monte-Carlo scheme to predict the shape of the intermittent stress-strain curve associated with microcrystal deformation by emulating the progressive activation and exhaustion of the weakest sources (12). The model assumes that plastic deformation occurs only via strain bursts and, it requires a priori knowledge of selected characteristics of intermittent flow behavior, such as the survival probability of occurrence for strain bursts that is both history- and stress-dependent, and for a given strain burst, the stress-dependent probability of the magnitude of the strain burst. While one can pass judgment on this study for using a purely ad hoc approach, the good qualitative agreement between the

simulated and experimental stress-strain curves indicates that continued investigation of the broad suite of intermittency characteristics is warranted.

Lastly, although not specifically addressing microcrystal deformation, the visionary paper by Sevillano and colleagues provides insight into another weak-link process that has not received much direct attention—the correlation length of the dislocation forest (84). In their classically-based description, this quantity is the characteristic distance between 'invading fingers' of a dislocation line that is gliding through a strong obstacle field, where the fingers correspond to relatively weaker regions of the dislocation forest. One can imagine that when the dimensions of the sample encroach upon this characteristic distance, the weakest-link paths for dislocations are modified and size-effects are observed. This study used simulations to calculate the correlation length in 2D for percolation through a point-obstacle array where only 20% of the forest obstacles are strong obstacles, and determined that the 2D correlation length was approximately equal to $27(\rho)^{-\frac{1}{2}}$, where ρ is the total dislocation density. Notably, this approach provides a theoretical basis on which one can establish whether-or-not size effects should be observed and, this prediction agreed with the transition from bulk-like to size-affected behavior for experimental measurements of Ni microcrystals (25).

Furthermore, the Sevillano et al. study predicted that a size-dependent strengthening will be observed for samples below the correlation limit due to enhanced potency of the dislocation forest (weakest links are stochastically omitted), and these predictions also agreed with experimental measurements (25). This study also predicted a decrease in the Stage II strain-hardening rate with decreasing crystal size that remains to be investigated. However, the study never considered the initial modifications to the initial source lengths from free surface interactions, nor did it fully envisage the potent strain-hardening response in the small-strain regime observed in experiments. Nonetheless, the visionary concepts contained in this model should be further explored, especially by state-of-the-art 3D DDS.

Concluding Remarks

Taken as a whole, the microcompression experiments, simulations, and associated theory have—in our opinion—made the following contributions to the scientific study of dislocation-based deformation processes. First, there is now clear evidence that size-scale effects exist independently of other known size-dependent strengthening effects such as nucleation-controlled deformation (whiskers) or the presence of imposed strain gradients. While size-dependent strengthening has often been measured in metallic thin-films, the microcompression experiments discussed herein were largely performed on single-crystal samples, thus removing complications associated with strengthening due to either grain boundaries or an underlying substrate. However, many unbounded or unanswered questions regarding these phenomena remain, such as:
- What size and internal structure leads to the strongest materials?
- For what size and internal structure should one observe a transition from bulk behavior?

- What will the study of isolated micro-mechanisms in small samples ultimately teach us about bulk-sample behavior?
- How do mechanisms such as thermal activation affect the size-dependent response?
- How do these scale-dependent mechanisms affect creep, fatigue, and fracture processes?

Second, this methodology provides a ready means to explore the fundamentals of deformation processes. Small samples can be carved from a bulk monolithic material with great control over the size and location of the test volume. A suite of samples can be tested in a uniform manner, thereby allowing one to discern changes in properties simply due to either changes in the size of the test sample, the starting internal structure, or the test conditions. In addition, the diminutive test volume enables advanced simulation methods to mimic as much as possible the exact test sample and associated boundary conditions.

Third, the small volume of the samples facilitates the measurement of stochastic dislocation activity by permitting the isolated measurement of discrete slip events, thereby enabling the direct measurement of the magnitude, duration, and the time between slip events. These measurements are likely a fruitful area for understanding how dislocation ensembles dissipate energy, and hopefully will help advance new meso-scale theories that predict plastic deformation.

With continued effort, we envisage that this type of experimental methodology will allow one to locally determine the full suite of properties of various microconstituents (phases, precipitates) in fully-processed engineering materials. There remains practical challenges in the area of sample fabrication and testing, such as transitioning from serial to parallelized fabrication methods that are generically applicable and, in performing a more rich palette of testing modes (tension (Kiener Acta 2008), for example) whilst providing as much information on the internal structural changes as possible. Similar challenges exist within modeling and simulation, such as incorporating realistic starting dislocation networks or internal microstructural features and, being able to simulate 'larger' volumes to bridge the gap between micro- and mesoscopic deformation.

Literature Cited

1. Uchic MD, Dimiduk DM, Florando JN, Nix WD. 2003. Exploring specimen size effects in plastic deformation of $Ni_3(Al, Ta)$. *Mater. Res. Soc. Symp. Proc.* 753:BB1.4.1-6

2.	Uchic MD, Dimiduk DM, Florando JN, Nix WD. 2004. Sample dimensions influence strength and crystal plasticity. *Science* 305:986-989

3.	Uchic MD, Dimiduk DM. 2005. A methodology to investigate size scale effects in crystalline plasticity using uniaxial compression testing. *Mater. Sci. Eng. A* 400-401:268-278

4.	Greer JR, Nix WD. 2006. Nanoscale gold pillars strengthened through dislocation starvation. *Phys. Rev. B* 73:245410

5.	Moser B, Wasmer K, Barbieri L, Michler J. Strength and fracture of Si micropillars: a new scanning electron microscopy-based micro-compression test. *J. Mater. Res.* 22:1004-1011

6.	Bei H, Shim S, George EP, Miller MK, Herbert EG, Pharr GM. 2007. Compressive strengths of molybdenum alloy micro-pillars prepared using a new technique. *Scripta Mater.* 57:397-400

7.	Greer JR, Oliver WC, Nix WD. 2005. Size dependence of mechanical properties of gold at the micron scale in the absence of strain gradients. *Acta Mater.* 53:1821-1830
	Erratum. 2006. *Acta Mater.* 54:1705

8.	Greer JR, Nix WD. 2005. Size dependence of mechanical properties of gold at the sub-micron scale. *Appl. Phys. A* 80:1625-1629
	Erratum. 2008. *Appl. Phys. A* 90:203

9.	Volkert CA, Lilleodden ET. 2006. Size effects in the deformation of sub-micron Au columns. *Phil. Mag.* 86:5567-5579

10.	Frick CP, Orso S, Arzt E. 2007. Loss of pseudoelasticity in nickel-titanium sub-micron compression pillars. *Acta Mater.* 55:3845-3855

11.	Shan ZW, Mishra RK, Syed Asif SA, Warren OL, Minor AM. 2008. Mechanical annealing and source-limited deformation in submicrometre-diameter Ni crystals. *Nature Mater.* 7:115-119

12.	Ng KS, Ngan AHW. 2008. Stochastic nature of plasticity of aluminum micro-pillars. *Acta Mater.* 1712-1720

13.	Zhang H, Schuster BE, Wei Q, Ramesh KT. 2006. The design of accurate micro-compression experiments. *Scripta Mater.* 54:181-186

14.	Volkert CA, Minor AM. 2007. Focused ion beam microscopy and micromachining. *MRS Bulletin* 32:389-395

15.	Orloff J, Utlaut M, Swanson L. 2003. *High Resolution Focused Ion Beams: FIB and Its Applications*. New York, NY: Kluwer Academic/Plenum Publishers

16.	Kiener D, Motz C, Rester M, Jenko M, Dehm G. 2007. FIB damage of Cu and possible consequences for miniaturized mechanical tests. *Mater. Sci. Eng. A* 459:262-272

17.	Genc A, Williams REA, Huber DE, Fraser HL. 2008. Some practical aspects of focused ion beam sample preparation for transmission electron microscopy. Submitted for publication.

18.	Marien J, Plitzko JM, Spolenak R, Keller RM, Mayer J. 1999. Quantitative electron spectroscopic imaging studies of microelectronic metallization layers. *J. Microscopy* 194:71-78

19. Yu J, Liu J, Zhang J, Wu J. 2006. TEM investigation of FIB induced damages in preparation of metal material TEM specimens by FIB. *Mater. Lett.* 60:206-209

20. Motz C, Schoberl T, Pippan R. 2005. Mechanical properties of micro-sized copper bending beams machined by the focused ion beam technique. *Acta Mater.* 53:4269-4279

21. Bei H, Shim S, Miller MK, Pharr GM, George EP. 2007. Effects of focused ion beam milling on the nanomechanical behavior of a molybdenum-alloy single crystal. *Appl. Phys. Lett.* 91:111915

22. Choi YS, Uchic MD, Parthasarathy TA, Dimiduk DM. 2007. Numerical study on microcompression tests of anisotropic single crystals. *Scripta Mater.* 57:849-852

23. Shade PA, Wheeler R, Choi YS, Uchic MD, Dimiduk DM, Fraser HL. 2008. A combined experimental and computational study to examine lateral constraint effects on single-slip oriented microcompression experiments. Unpublished research.

24. Raabe D, Ma D, Roters F. 2007. Effects of initial orientation, sample geometry and friction on anisotropy and crystallographic orientation changes in single crystal microcompression deformation: a crystal plasticity finite element study. *Acta Mater.* 55:4567-4583

25. Dimiduk DM, Uchic MD, Parthasarathy TA. 2005. Size-affected single-slip behavior of pure nickel microcrystals. *Acta Mater.* 53:4065-4077

26. Schuh CA, Mason JK, Lund AC. 2005. Quantitative insight into dislocation nucleation from high-temperature nanoindentation experiments. *Nature Mater.* 4:617-621

27. Frick CP, Clark BG, Orso S, Schneider AS, Arzt E. 2008. Size effect on strength and strain hardening of small-scale [1 1 1] nickel compression pillars. *Mater. Sci. Eng. A* 489:319-329

28. Kraft O, Volkert CA. 2006. Size effects on deformation and fatigue of thin films and small structures. Presented at CAMTEC, Cambridge University, UK.

29. Kiener D. 2007. *Size effects in single crystal plasticity of copper under uniaxial loading.* Dissertation. University of Leoben, Austria

30. Kiener D, Motz C, Schoberl T, Jenko M, Dehm G. 2006. Determination of mechanical properties of copper at the micron scale. *Adv. Eng. Mater.* 8:1119-1125

31. Brinckmann S, Kim JY, Greer JR. 2008. Fundamental differences in mechanical behavior between two types of crystals at the nanoscale. *Phys. Rev. Lett.* 100:155502

32. Bei H, Shim S, Pharr GM, George EP. 2008. Effects of pre-strain on the compressive stress-strain response of Mo-alloy single-crystal micropillars. *Acta Mater.* 56:4762-4770

33. Rao SI, Dimiduk DM, Parthasarathy, TA, Uchic MD, Tang M, Woodward C. 2008. Athermal mechanisms of size-dependent crystal flow gleaned from three-dimensional discrete dislocation simulations. *Acta Mater.* 56:3245-3259

34. Norfleet DM, Dimiduk DM, Polasik SJ, Uchic MD, Mills MJ. 2008. Dislocation structures and their relationship to strength in deformed nickel microcrystals. *Acta Mater.* 56:2988-3001

35 Greer JR, Weinberger CR, Cai W. 2008. Comparing the strength of f.c.c. and b.c.c. sub-micrometer pillars: compression experiments and dislocation dynamics simulations. *Mater. Sci. Eng. A* 493:21-25

35. Zaiser M, Schwerdtfeger J, Schneider AS, Frick CP, Clark BG, et al. 2008. Strain bursts in plastically deforming molybdenum micro- and nanopillars. *arXiv.org* arXiv:0802.1843v1

36. Uchic MD, Florando JM, Dimiduk DM. Unpublished research

37. Nadgorny EM, Dimiduk DM, Uchic MD. 2007. Size effects in LiF micron-scale single crystals of low dislocation density. *Mater. Res. Soc. Symp. Proc.* 976:EE06-24

38. Nadgorny EM, Dimiduk DM, Uchic MD. 2008. Size effects in LiF micron-scale single crystals of low dislocation density. *J. Mater. Res.* 23: In press

39. Frick CP, Clark BG, Orso S, Sonnweber-Ribic P, Arzt E. 2008. Orientation-independent pseudoelasticity in small-scale NiTi compression pillars. *Scripta Mater.* 59:7-10

40. Norfleet DM. 2007. *Sample size effects related to nickel, titanium and nickel-titanium at the micron size scale.* PhD Dissertation. The Ohio State University.

41. Polasik SJ. 2005. *Accelerated assessment and representation of materials behavior via integrated electron-optical, focused ion beam and MEMS-based characterization methods*. MS Thesis. The Ohio State University.

42. Dimiduk DM, Uchic MD, Rao SI, Woodward C, Parthasarathy TA. 2007. Overview of experiments on microcrystal plasticity in FCC-derivative materials: selected challenges for modeling and simulation of plasticity. *Model. Simul. Mater. Sci. Eng.* 15:135-146

43 Mara NA, Bhattacharyya D, Dickerson P, Hoagland RG, Misra A. 2008. Deformability of ultrahigh strength 5 nm Cu/Nb nanolayered composites. *Appl. Phys. Lett.* 92:231901

44. Rinaldi A, Peralta P, Friesen C, Sieradzki K. 2008. Sample-size effects in the yield behavior of nanocrystalline nickel. *Acta Mater.* 56:511-517

45. Schuster BE, Wei Q, Zhang H, Ramesh KT. 2006. Microcompression of nanocrystalline nickel. *Appl. Phys. Lett.* 88:103112

46. Lai YH, Lee CJ, Cheng YT, Chou HS, Chen HM, et al. 2008. Bulk and microscale compressive behavior of a Zr-based metallic glass. *Scripta Mater.* 58:890-893

47. Volkert CA, Donohue A, Spaepen F. 2008. Effect of sample size on deformation in amorphous metals. *J. Appl. Phys.* 103:083539

48. Schuster BE, Wei Q, Hufnagel TC, Ramesh KT. 2008. Size-independent strength and deformation mode in compression of a Pd-based metallic glass. Submitted

49. Hosemann P, Swadener JG, Kiener D, Was GS, Maloy SA, Li N. 2008. An exploratory study to determine applicability of nano-hardness and micro-compression measurements for yield stress estimation. *J. Nucl. Mater.* 375:135-143

50. Volkert CA, Lilleodden ET, Kramer D, Weissmüller. 2006. Approaching the theoretical strength in nanoporous Au. *Appl. Phys. Lett*. 89:061920

51. Michler J, Wasmer K, Meier S, Ostlund F, Leifer K. 2007. Plastic deformation of gallium arsenide micropillars under uniaxial compression at room temperature. *Appl. Phys. Lett.* 90:043123

52. Ng KS and Ngan AHW. 2007. Creep of micron-sized aluminum columns. *Philos. Mag. Lett*. 87:967-977

53. Motz C, Weygand D, Senger J, Gumbsch P. 2008. Micro-bending tests: a comparison between three-dimensional discrete dislocation dynamics simulations and experiments. *Acta Mater.* 56:1942-1955

54. Kiener D, Grosinger W, Dehm G, Pippan R. 2008. A further step towards an understanding of size-dependent crystal plasticity: in situ tension experiments of miniaturized single-crystal copper samples. *Acta Mater.* 56:580-592

55. Dimiduk DM, Woodward C, LeSar R, Uchic MD. 2006. Scale-free intermittent flow in crystal plasticity. *Science* 312:1188-1190

56. Pond RB. 1973. In *The Inhomogeneity of Plastic Deformation*, pp. 1-18. Metals Park, OH: American Society for Metals

57. Weiss J, Marsan D. 2003. Three-dimensional mapping of dislocation avalanches: clustering and space/time coupling. *Science* 299:89-92

58. Csikor FF, Motz C, Weygand D, Zaiser M, Zapperi S. 2007. Dislocation avalanches, strain bursts, and the problem of plastic forming at the micrometer scale. *Science* 318:251-254

59. Ng KS, Ngan AHW. 2008. A Monte Carlo model for the intermittent plasticity of micro-pillars. *Model. Simul. Mater. Sci. Eng.* 16:055004

60. Ng KS, Ngan AHW. 2008. Stochastic theory for jerky deformation in small crystal volumes with pre-existing dislocations. *Phil. Mag.* 88:677-688

61 . Dimiduk DM, Woodward C, Uchic MD. Unpublished research.

62. Norfleet DM, Dimiduk DM, Uchic MD, Mills MJ. Unpublished research.

63. Budiman AS, Han SM, Greer JR, Tamura N, Patel JR, Nix WD. 2008. A search for evidence of strain gradient hardening in Au submicron pillars under uniaxial compression using synchrotron x-ray microdiffraction. *Acta Mater.* 56:602-608

64. Maass R, Grolimund D, Van Petegem S, Willimann M, Jensen M, et al. 2006. Defect structure in micropillars using x-ray microdiffraction. *Appl. Phys. Lett.* 89:151905

65. Maass R, Van Petegem S, Zimmermann J, Borca CN, Van Swygenhoven H. 2008. On the initial microstructure of metallic micropillars. *Scripta Mater.* 59:471-474

66. Maass R, Van Petegem S, Grolimund D, Van Swygenhoven H, Uchic MD. 2007. A strong micropillar containing a low angle grain boundary. *Appl. Phys. Lett.* 91:131909

67. Maass R, Van Petegem S, Van Swygenhoven H, Derlet PM, Volkert CA, Grolimund D. 2007. Time-resolved Laue diffraction of deforming micropillars. *Phys. Rev. Lett.* 99:145505

68. Maass R, Van Petegem S, Grolimund D, Van Swygenhoven H, Kiener D, Dehm G. 2008. Crystal rotation in Cu single crystal micropillars: in situ Laue and electron backscatter diffraction. *Appl. Phys. Lett.* 92:071905

69. Shade PA, Uchic MD, Dimiduk DM, Fraser HL. Unpublished research

70. Greer JR, Nix WD. 2006. Nanoscale gold pillars strengthened through dislocation starvation. *Phys. Rev. B* (EPAPS):E-PRBMDO-73-061624

71. Greer, JR. 2006. Bridging the Gap Between Computation and Experimental Length Scales: A Review on Nano-Scale Plastisicy. *Rev. Adv. Mater. Sci* 13:59-70

72. Van der Giessen E, Needleman A. 1995. Discrete dislocation plasticity: a simple planar model. *Model. Simul. Mater. Sci. Eng.* 3:689-735

73. Deshpande VS, Needleman A, Van der Giessen E. 2005. Plasticity size effects in tension and compression of single crystals. *J. Mech. Phys. Solids* 53:2661-91

74. Deshpande VS, Needleman A, Van der Giessen E. 2005. Discrete dislocation plasticity analysis of single slip tension. *Mater. Sci. Eng. A* 400-401:154-57

75. Balint DS, Deshpande VS, Needleman A, Van der Giessen E. 2006. Size effects in uniaxial deformation of single and polycrystals: a discrete dislocation plasticity analysis. *Model. Simul. Mater. Sci. Eng.* 14:409-422

76. Benzerga AA, Shaver NF. 2006. Scale dependence of mechanical properties of single crystals under uniform deformation. *Scripta Mater.* 54:1937-1941

77. Guruprasad PJ, Benzerga AA. 2008. Size effects under homogeneous deformation of single crystals: a discrete dislocation analysis. *J. Mech. Phys. Solids* 56:132-156

78. Tang H, Schwarz KW, Espinosa HD. 2007. Dislocation escape-related size effects in single-crystal micropillars under uniaxial compression. *Acta Mater.* 55:1607-1616

79. Rao SI, Dimiduk DM, Tang M, Parthasarathy TA, Uchic MD, Woodward C. 2007 Estimating the strength of single-ended dislocation sources in micron-sized single crystals. *Phil. Mag.* 87:4777-4794

80. Weygand D, Poignant M, Gumbsch P, Kraft O. 2008. Three-dimensional dislocation dynamics simulation of the influence of sample size on the stress-strain behavior of fcc single-crystalline pillars. *Mater. Sci. Eng. A* 483:188-190

81. El-Awady J, Biner SB, Ghoniem NM. 2008. A self-consistent boundary element, parametric dislocation dynamics formulation of plastic flow in finite volumes. *J. Mech. Phys. Solids* 56:2019-2035.

82. Senger J, Weygand D, Gumbsch P, Kraft O. 2008. Discrete dislocation simulations of the plasticity of micro-pillars under uniaxial loading. *Scripta Mater.* 58:587-90

83. Tang H, Schwarz KW, Espinosa HD. 2008. Dislocation-source shutdown and the plastic behavior of single-crystal micropillars. *Phys. Rev. Lett.* 100:185503

84. Gil Sevillano J, Ocana Arizcorreta I, Kubin LP. 2001. Intrinsic size effects in plasticity by dislocation glide. *Mater. Sci. Eng. A* 309-310:393-405

85. Berdichevsky VL. 2006. On thermodynamics of crystal plasticity. *Scripta Mater.* 54:711-716

86.   Parthasarathy TA, Rao SI, Dimiduk DM, Uchic MD, Trinkle DR. 2007. Contributions to size effect of yield strength from the stochastics of dislocation source lengths in finite samples. *Scripta Mater.* 56:313-316

87.   Ng KS, Ngan AHW. 2008. Breakdown of Schmid's law in micropillars. *Scripta Mater.* 59:796-799

Figure Captions

1. (a) Schematic of the microcompression test (b) schematic of the flow response of a microcrystal oriented for single slip, see (25) for details (c) scanning electron image of a 5 micrometer diameter microcrystal sample of pure Ni oriented for single slip (d) SEM image of (c) after testing.   Figure is adapted from reference (25).

2. Experimental flow curves for two 10 micrometer diameter nickel-base superalloy microcrystals, where the lateral constraint has been varied significantly between the two experiments. The change in lateral constraint has a demonstrable effect on the flow curves, and for the highly constrained sample, results in significant internal gradients within the sample as shown in the accompanying Electron Backscatter Diffraction Maps. Figure is adapted from reference (23).

3. Composite plot of published microcrystal flow stress data as a function of sample diameter for FCC metals. Data in the plot have been normalized by the shear modulus and Burger's vector. The scaling exponent *n* that best fits the data is approximately 0.6.

4. Representative experimental flow curves for pure molybdenum <2 9 20>-oriented microcrystals that clearly demonstrate size-dependent strengthening effects (36).

5. Experimental flow stress data for Mo solid solution microcrystals, some of which have varying degrees of initial dislocation density due to pre-straining experiments. Figure is from reference (32). See text for an explanation of this figure.

6. (a) A collection of flow curves from 20 micrometer diameter Ni microcrystals with a <2 6 9> orientation that display flow intermittency (strain bursts) (b) the event frequency distribution showing the number of slip events n(x), versus event size, x, plotted on logarithmic scales. Power law scaling over more than two orders of magnitude is exhibited for both a single sample (open circles) and the aggregate date from several samples (solid circles). Figure is from reference (55).

7. (a) Composite plot of published simulation flow stress data as a function of simulation cell size. Data in the plot have been normalized by the shear modulus and Burger's vector. The light blue area designates the range of experimental measurements shown in Fig. 3. (b) subset of data in (a), demonstrating the effect of the initial starting density on the size-scaling behavior and resulting scaling exponent.

8. Predictions of the Parthasarathy et al. model for (a) nickel and (b) gold, shown in comparison with reported experimental data (from references (2,7,8,9,25). The dotted green and red lines correspond to the lower and upper standard deviations from the mean as predicted by the model. Figure is adapted from reference (86).

9. Yield probability versus diameter for activity on the four possible slip planes for [3 -1 5] oriented Al microcrystals, plotted together with experimental measurements of slip trace activity at small strains. Figure is from reference (87).

a

Voice Coil

Capacitive
Displacement
Sensor

Diamond Tip

Sample

b

P

φ

D

dL

θ

u'

L_o

h_o

slip
zone

c

5 μm #2

4 μm

d

5 μm #2

4 μm

Figure 1

28
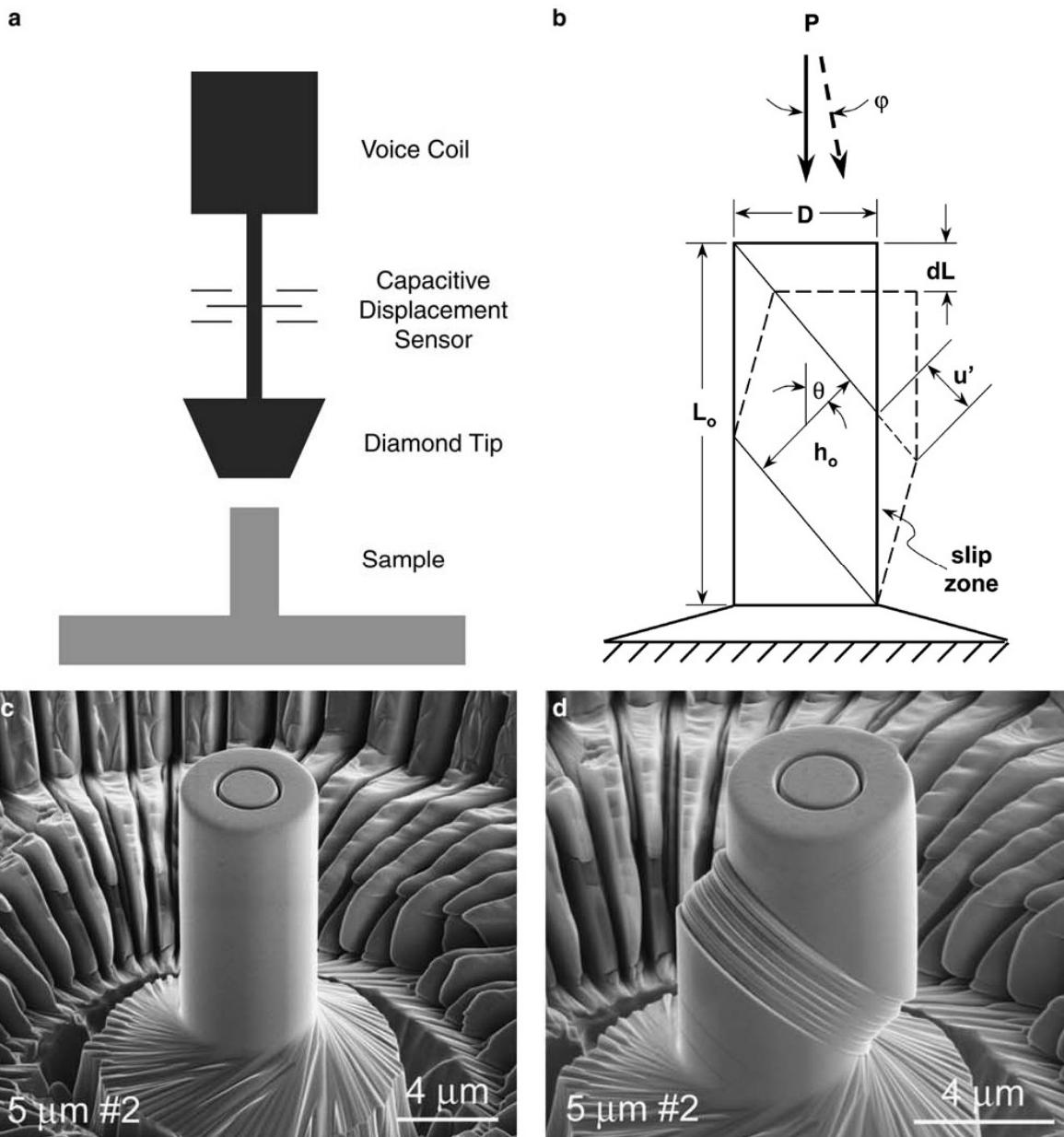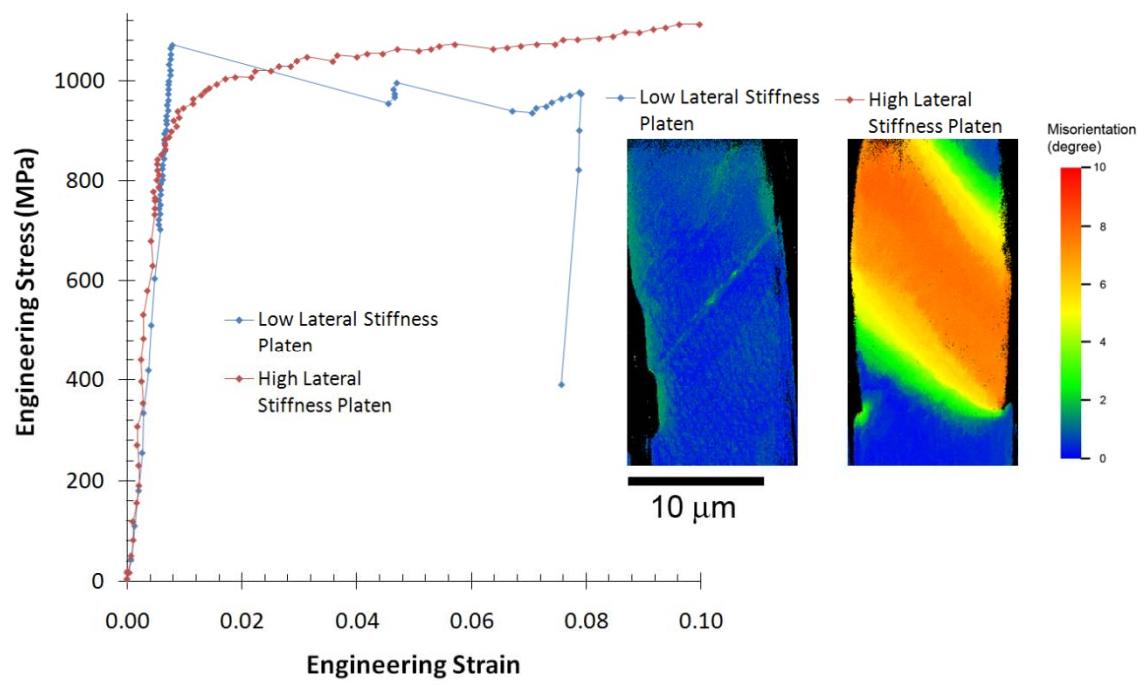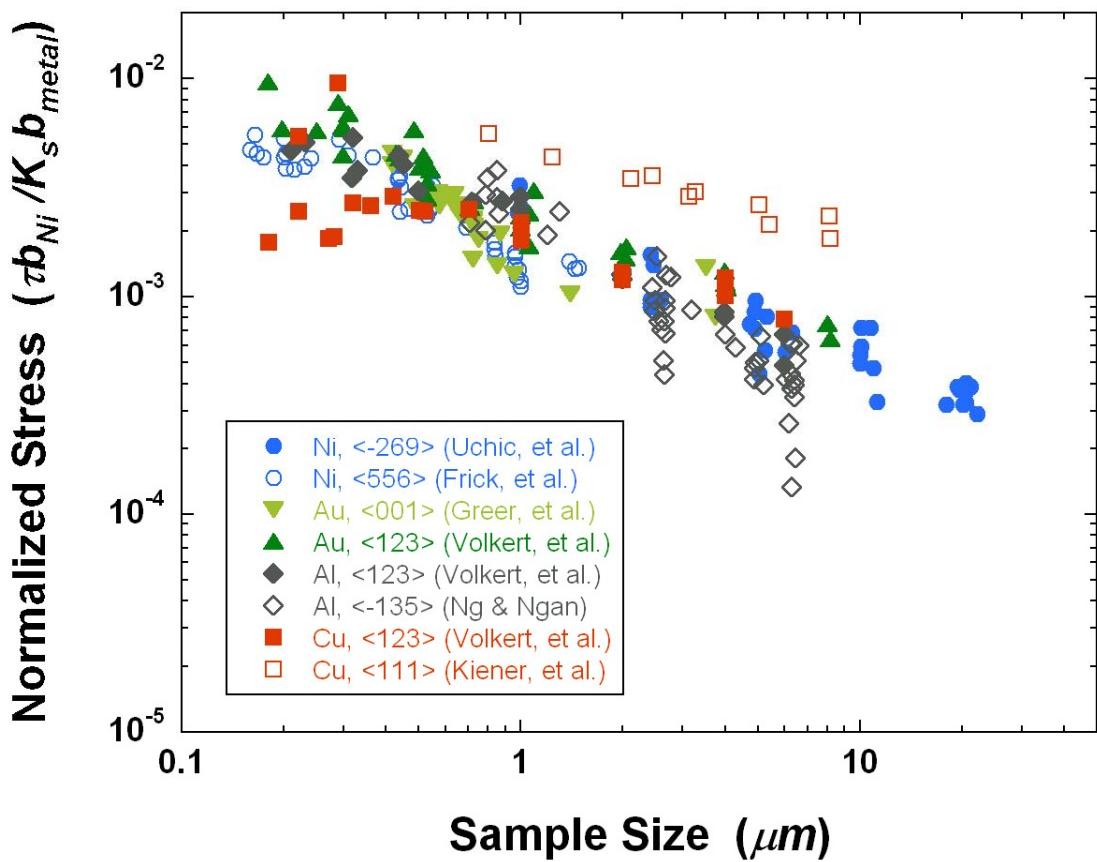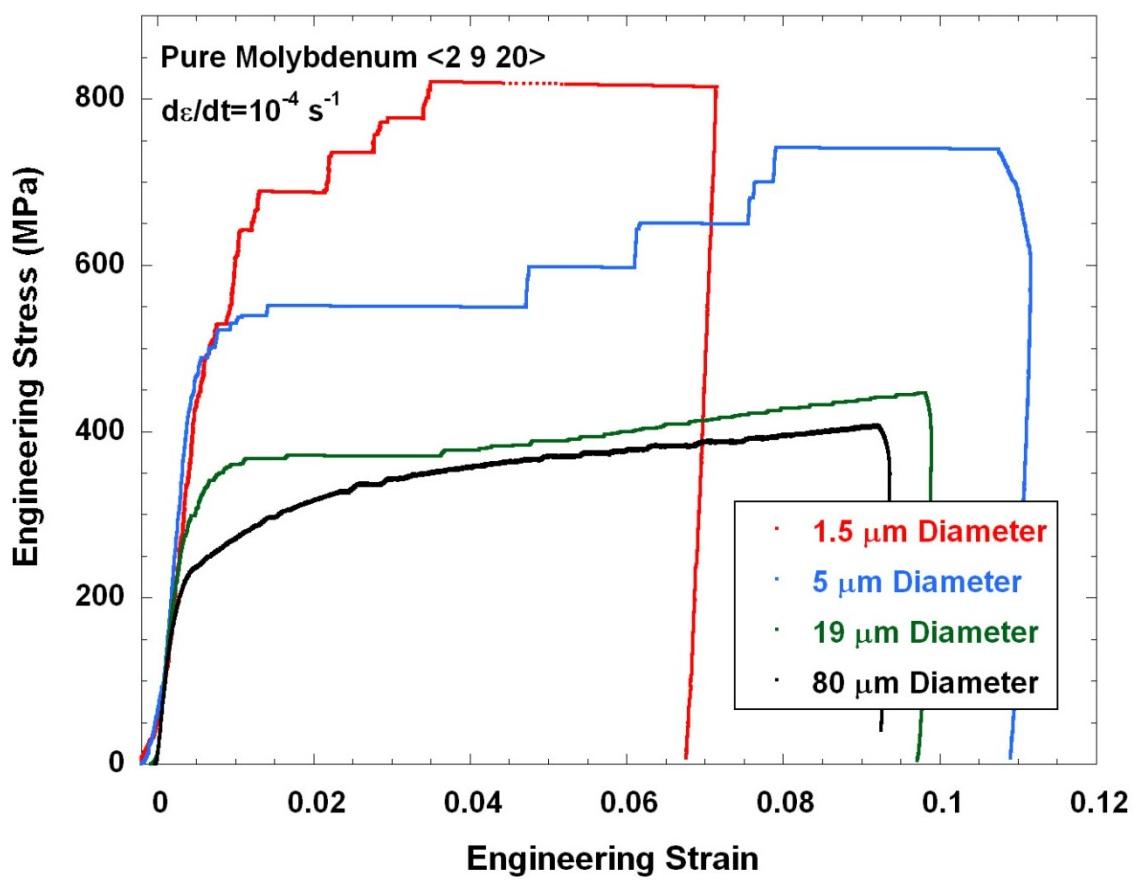
Figure 2

Figure 3

Figure 4
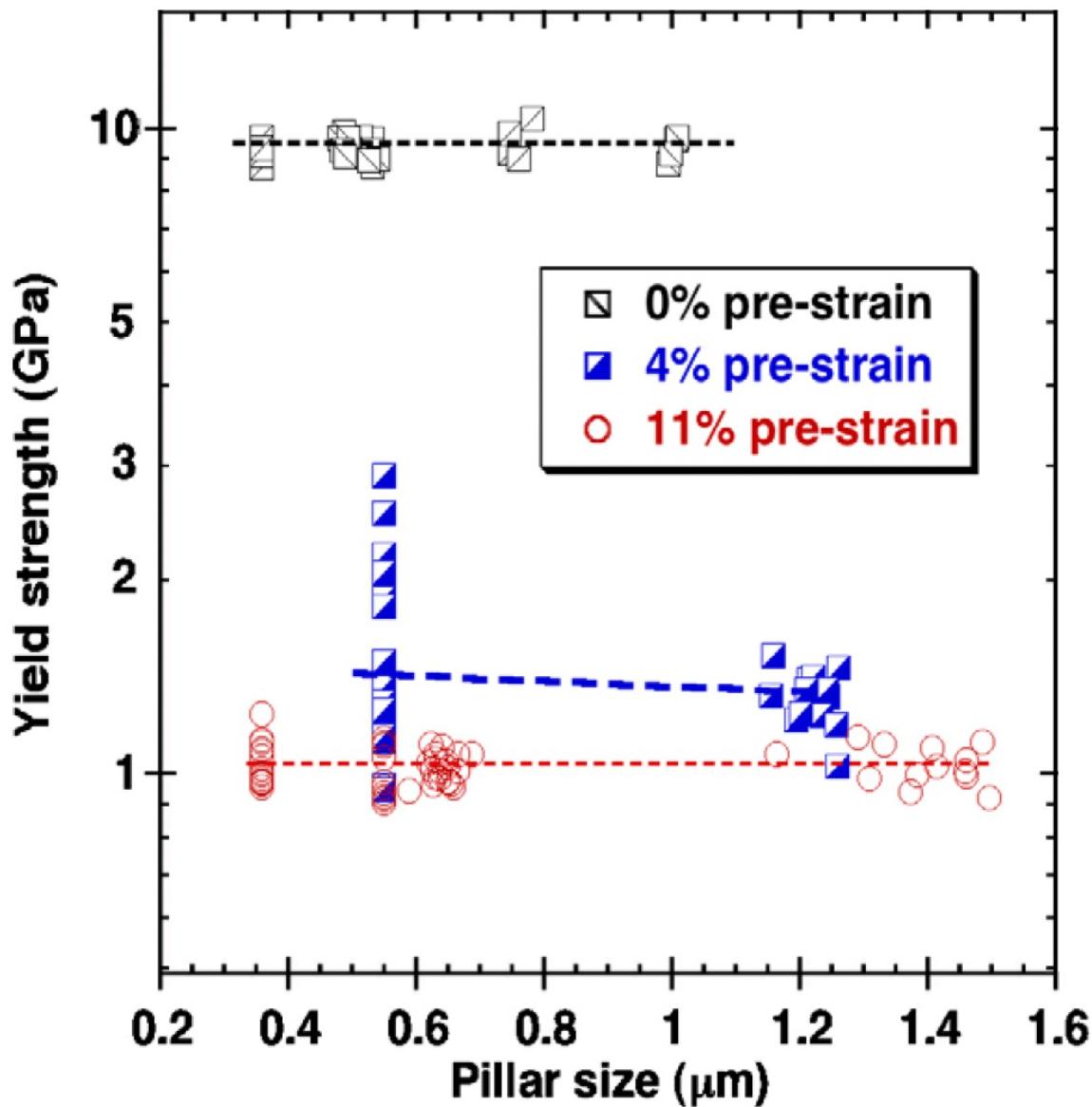
Figure 5

Figure 6

Figure 7

Figure 8

Figure 9